LA--12485-M

DE93 006378

# *PFPF Canister Counter for Foreign Plutonium (PCAS-3) Hardware Operations and Procedures Manual*

*H. O. Menlove*
*J. Baca*
*K. E Kroncke*
*M. C. Miller*
*S. Takahashi**
*S. Seki**
*S. Inose**
*T. Yamamoto**

**Tokai-Mura Naka-Gun, Ibaraki-Ken, JAPAN*



Los Alamos
NATIONAL LABORATORY
Los Alamos, New Mexico 87545

## CONTENTS

# PFPF CANISTER COUNTER FOR FOREIGN PLUTONIUM (PCAS-3) HARDWARE OPERATIONS AND PROCEDURES MANUAL

by

H. O. Menlove, J. Baca, K. E. Kroncke, M. C. Miller,
S. Takahashi, S. Seki, S. Inose, and T. Yamamoto

## ABSTRACT

A neutron coincidence counter has been designed for the measurement of plutonium powder contained in tall storage canisters. The counter was designed for installation in the Plutonium Fuel Production Facility fabrication plant. Each canister contains from one to five cans of $PuO_2$. The neutron counter measures the spontaneous-fission rate from the plutonium and, when this is combined with the plutonium isotopic ratios, the plutonium mass is determined. The system can accommodate plutonium loadings up to 12 kg, with 10 kg being a typical loading. Software has been developed to permit the continuous operation of the system in an unattended mode. Authentication techniques have been developed for the system. This manual describes the system and its operation and gives performance and calibration parameters for typical applications.

## GENERAL

We have designed a neutron coincidence counter to verify the amount of plutonium in storage canisters. This plutonium canister assay system (PCAS-3) was designed to be installed in the Plutonium Fuel Production Facility (PFPF) operated by the Power Reactor & Nuclear Fuel Development Corporation (PNC) in Japan. The detector will be located in the storage area for foreign-origin canisters at PFPF. The system consists of

- detector head,
- security cap,
- electronics cabinet,
- JSR-II coincidence counting electronics (2),
- COMPAQ III portable computers (2), and
- Epson LQ-850 printer.

The duplicate electronic components in the cabinet operate independently and in parallel to increase the reliability of the system. However, the high voltage (hv) and 5 V for the detector head come exclusively from unit A, so no redundancy is provided for these supplies. Spare units are provided for the JSR-11 and the COMPAQ III Portable Computer.

The electronics of the PCAS-3 are similar to those of the High-Level Neutron Coincidence Counter (HLNC-II).[1,2] The detector counts the totals and coincidence neutrons from the spontaneous fission of the even isotopes of plutonium.

The design-basis samples are canisters that contain up to 10 kg of $PuO_2$ in four or five separate cans. These cans are stacked on top of each other inside the canister that is used to transfer and store the plutonium.

An earlier version of a canister counter[3] was built in 1989, but for a different size canister and lower plutonium loadings. Both systems were designed for unattended operation.

**GENERAL (cont.)**

This manual describes the components, performance characteristics, and operating procedures for the canister counter.

**DETECTOR BODY**

To accommodate the shape and height of the sample container (canister), it was necessary to design the PCAS-3 body to fit around a concrete shield provided by PFPF. The detector fits on the outside of the central concrete shield as shown in Fig. 1.

For handling safety reasons, the canister never touches the PCAS-3 during insertion, measurement, and removal. The

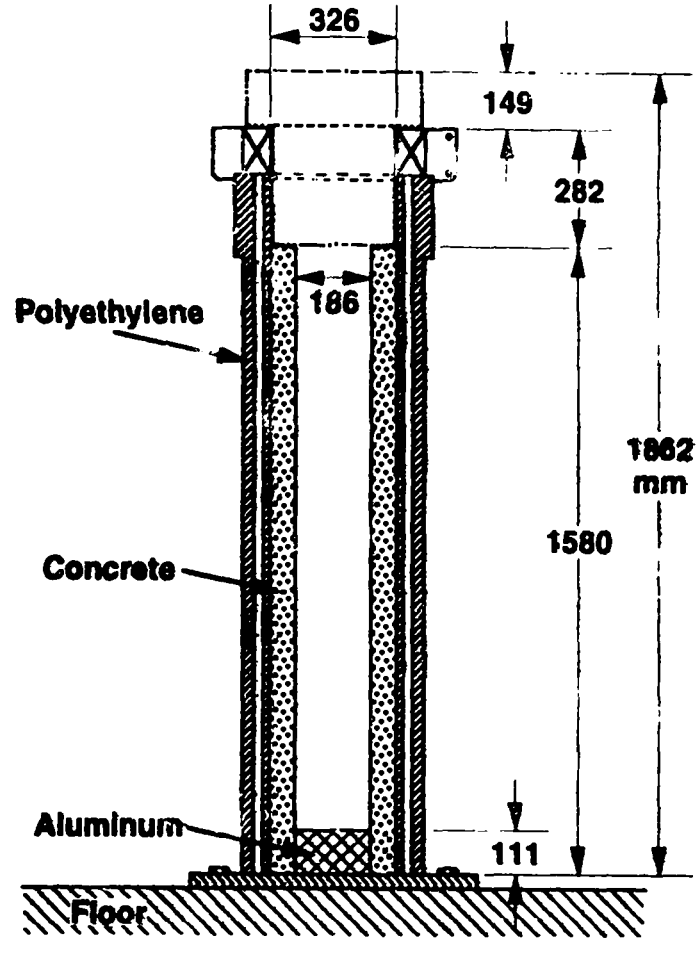


*Fig. 1. Schematic diagram of concrete shield and PCAS-3 detector body with the central cavity for the canister.*

**DETECTOR BODY**
**(cont.)**

entire canister weight is supported by the concrete pillar in the center of the detector. The canister seat and concrete were supplied by PNC. Figure 2 shows the detector with the top removed and the $^{3}He$ tubes partially withdrawn from the polyethylene body.

The canister is lowered into the detector by an automated overhead manipulator. Figure 3 shows the top of the counter with the security cover over the electronics and detector head. Figure 4 shows the assembled system.

The PCAS-3 detector is placed around the concrete shield with the AMPTEK electronics and the hv junction box at the top of the detector. The requirement for a flat axial

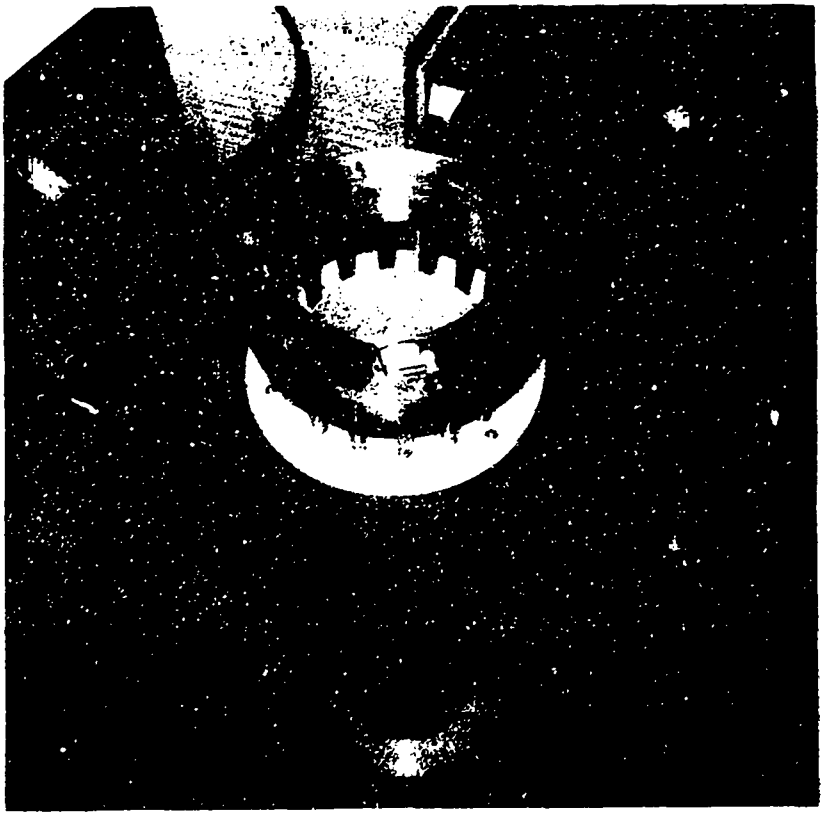

*Fig. 2. The PCAS-3 detector with the electronics cover removed to show the AMPTEK amplifiers and the $^{3}He$ tubes partially withdrawn from the polyethylene body.*

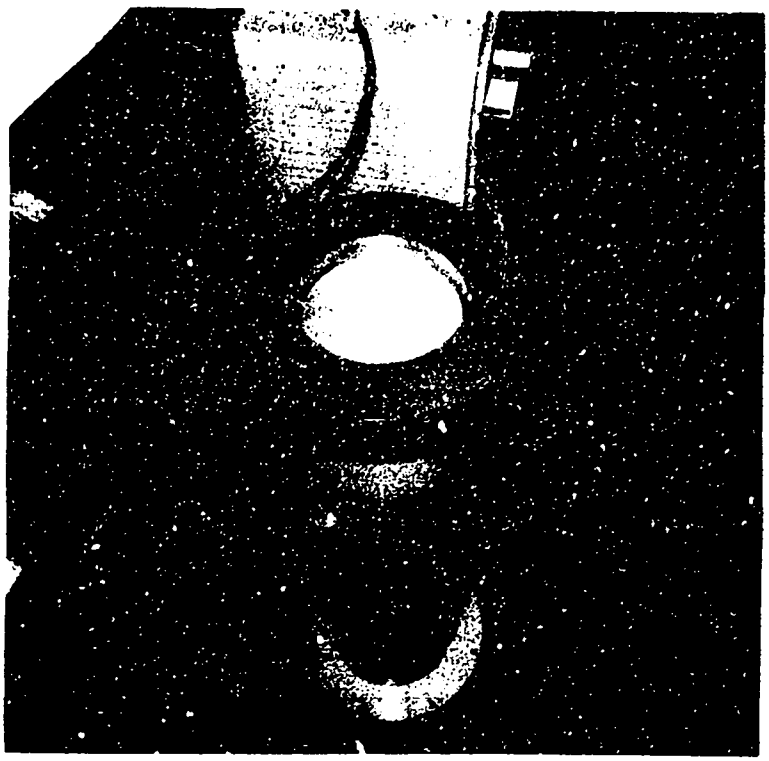

*Fig. 3. Top view of PCAS-3 showing the detector body and security cover for the electronics.*

*Fig. 4. The assembled PCAS-3 detector surrounding the concrete pedestal.*

**DETECTOR BODY**
**(cont.)**

response in the detector necessitated putting as much neutron-detection efficiency as possible in the top section of the detector to compensate for the leakage of neutrons out of the top of the detector.

At the bottom of the canister, an aluminum plug reflects neutrons back into the detector zone. Again, this placement helps flatten the axial neutron profile.

At the interface of the inside of the polyethylene detector and the concrete annulus, there are custom-tailored cadmium absorbers (0.4-mm thick) to help flatten the axial response profile. The size and location of the cadmium is given in Fig. 5. Also, there is a strip of cadmium on the

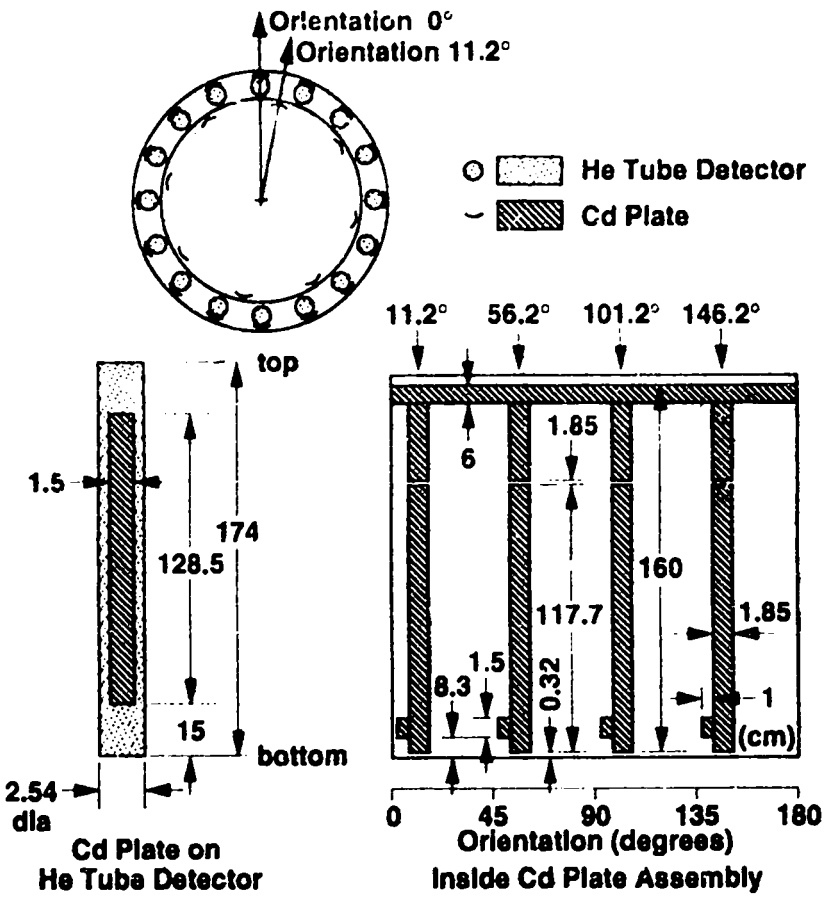


*Fig. 5. Diagrams of the cadmium locations on the $^3He$ tubes and the stainless steel liner between the $CH_2$ and concrete.*

**DETECTOR BODY (cont.)**

central portion of each $^{3}He$ tube to help flatten the axial response profile.

The detector body, including the hv junction box, has a mass of ~140 kg. There are three lifting bolts at the top of the unit for attaching to an overhead crane or forklift.

**SECURITY COVER**

A top cover is provided to protect the detector head and electronics. This cover, shown in Fig. 3, contains the inspector's seal to prevent undetected tampering with the detector head.

## CALIBRATION SOURCE

### System Check

A $^{252}Cf$ source was counted at the time of calibration and at each subsequent use of the detector for authentication purposes. A source with an initial emission rate of $8 \cdot 10^4$ n/s is adequate for at least 10 years of use in the canister counter. The initial reference sources used with the unit were CR-5 and K-189. Sources owned by the IAEA have been cross-calibrated with the CR-5 source. Table I gives the relative counting rates for all of the PFPF $^{252}Cf$ sources.

**TABLE I.** Californium-252 Source Ratios—PFPF (Data Updated to 92-01-01)

| Source | $\frac{Cf-x^a}{CR-5}$ | σ (%) | Activity (μCi) |
|---|---|---|---|
| K-181 | 3.731 | 0.03 | 8.1 |
| K-182 | 3.627 | 0.03 | 7.8 |
| K-183 | 3.490 | 0.08 | 7.5 |
| K-184 | 3.680 | 0.04 | 8.0 |
| K-185 | 3.527 | 0.08 | 7.6 |
| K-186 | 3.571 | 0.08 | 7.7 |
| K-187 | 7.054 | 0.08 | 15.2 |
| K-188 | 7.152 | 0.10 | 15.4 |
| K-189 | 7.194 | 0.03 | 15.5 |

[a]Source CR-5 gave $T$=2280 counts/s, $R$=488.1 counts/s (±0.02%), and an absolute yield of $0.9374 \cdot 10^4$ n/s (2.16 μCi) on 92-01-01.

The neutron sources check the system operation and can be used to normalize the calibration curve in the same manner as with the HLNC-II.

### Insertion

A neutron source holder consisting of a $CH_2$ plate attached to an aluminum rod to insert the source into the detector is supplied with the system. The source is positioned in the flat counting region of the detector by manual insertion from the top of the detector.

**Normalization**

The previously described source holder is used for manual system check-out and authentication. A second source is provided for automated use and normalization. This source is sealed in an otherwise empty canister.

The PFPF robotics system can automatically position this canister and source in the PCAS-3 for routine performance checks, control charting, and possible renormalization. Any renormalization of the calibration will be performed by a supervisor after reviewing the control chart data.

## DETECTOR TUBES

The PCAS-3 contains sixteen $^3$He tubes with the specifications listed in Table II. The tubes have been matched to have the same gain, efficiency, and operating hv.

**TABLE II.** Characteristics of $^3$He Tubes for PCAS-3[a]

| | |
|---|---|
| Tube model | RS-P4-0866-201 |
| Active length | 167.6 cm |
| Diameter | 2.5 cm |
| Fill pressure | 4 atm of helium |
| Gas quench | Argon + $CH_4$ |
| Cladding | Stainless steel |
| Operating hv | 1680 V |

[a]These $^3$He tubes have the same specifications as the Fuel Pin Assay System.

## ANALOG ELECTRONICS

The canister counter uses the new fast-counting circuitry[1] based on the miniature AMPTEK hybrid chip. These chips are located near the end of the $^3$He tubes (see Figs. 2 and 6) and contain the preamplifier, amplifier, and discriminator circuits. Eight of these amplifier units are located in the top part of the detector. The outputs of these eight amplifiers are added and sent to the input of the shift-register board. The connection is made through the "external SR input" on the back panel of the shift-register.

The status of the eight amplifier channels is indicated by eight signal lights connected to the outputs of the eight discriminators. These lights flash whenever the corresponding channel processes a discriminator output pulse. The $^3$He tube hv section of the detector is isolated from the AMPTEK amplifier board by the ground plate shown in Fig. 6.

## ANALOG ELECTRONICS
(cont.)

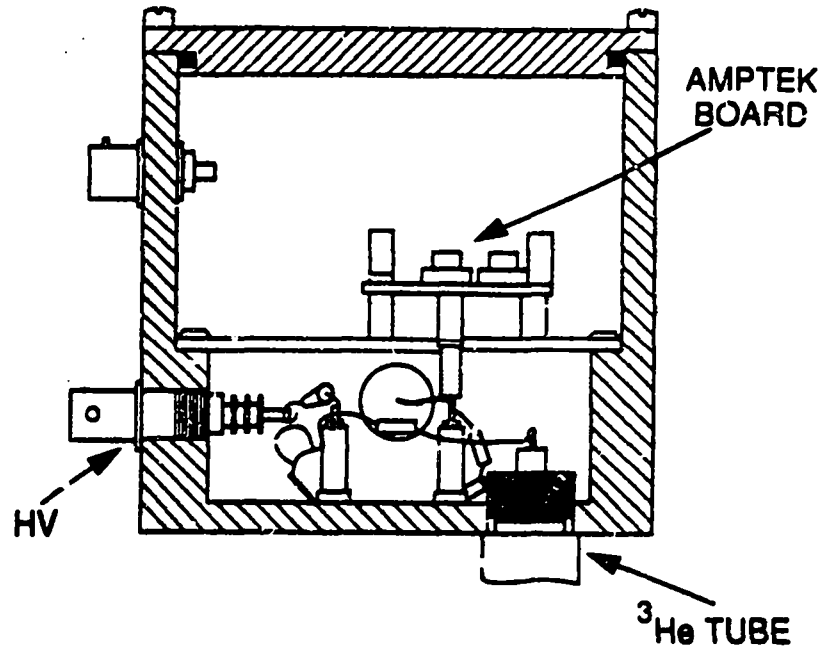


*Fig. 6. Diagram of a generic AMPTEK amplifier board in the hv junction box above the $^3$He tubes.*

The shift-register electronics* for the PCAS-3 is the same as that used for the upgraded HLNC-II.[2] The electronic modules and their connections in the cabinet are shown in Fig. 7. The signal splitter takes the input logic signal from the detector head and routes it to both JSR-11s for redundancy against component failure.

A second output from each computer is routed to the input trigger of the Sandia National Laboratory video camera that is used for determining the sample identification number.

### MOISTURE SEAL

To avoid moisture buildup in the hv junction box of the detector, we put desiccant in this space and sealed the openings with O-rings and silicone rubber. The humidity and degree of moisture saturation in the desiccant can be

*Model JSR-11, JOMAR Systems, Los Alamos, NM 87545.

**MOISTURE SEAL**
**(Cont.)**

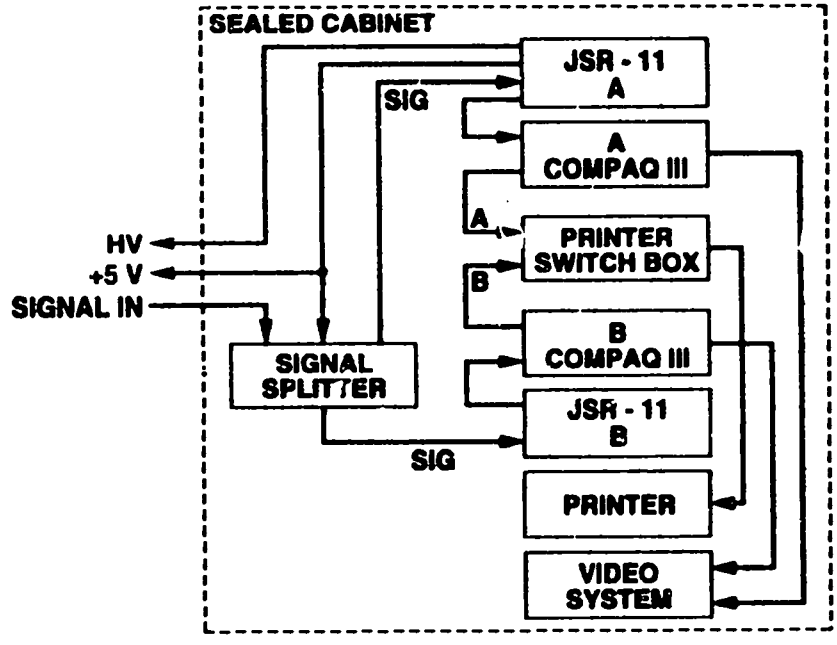


*Fig. 7. Connection of modules inside the electronics cabinet.*

read from outside the junction box. Also, the desiccant tubes can be exchanged for fresh tubes without removing the lid of the junction box. The procedures for this operation are described in the maintenance manual.

**HIGH-VOLTAGE PLATEAU**

Figure 8 shows the totals counting efficiency as a function of high-voltage setting. The operating voltage was set at 1680 V.

**HIGH-VOLTAGE PLATEAU**
**(cont.)**

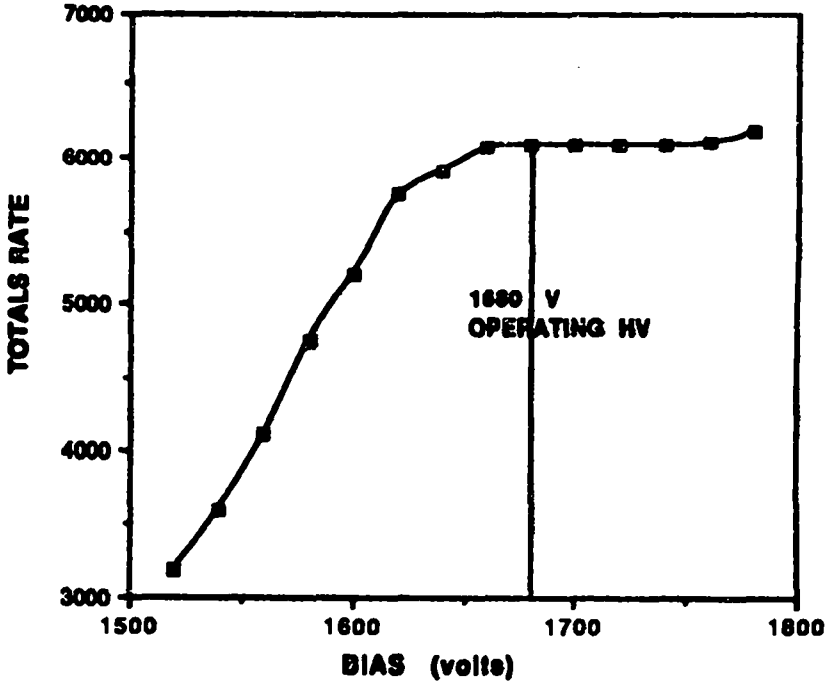


*Fig. 8. High-voltage plateau for the PCAS-3 detector.*

**EFFICIENCY**

The efficiency of the PCAS-3 system was measured using a calibrated $^{252}Cf$ source with a dummy canister in the detector. The results are listed in Table III.

**Table III. PCAS Performance Characteristics**

| Parameter | PCAS-3 |
|---|---|
| Efficiency (with canister) | 13.0% |
| Die-away time (center) | 52 μs |
| Gate setting | 64 μs |
| High voltage | 1680 V |
| Deadtime coefficient *a* | 0.690 μs |
| Deadtime coefficient *b* | 0.223 μs |

The detector plus the concrete wall thickness make the detector system slightly under moderated for fission spectrum neutrons. Thus, the addition of moisture to the sample matrix will increase the efficiency. This effect is described in the Matrix Effects section of this manual.

The proper gate setting in a neutron coincidence counter depends on the neutron die-away time ($\tau$) in the system. For minimum error, the coincidence gate length should be set equal to ~1.2 $\tau$ at high counting rates. A $^{252}Cf$ source was used to measure the die-away time, and the result was 52 μs in the central zone. We are using a gate setting of 64 μs.

**DETECTOR DEADTIME**

The canister counter uses the same basic electronics and amplifiers (eight channels—AMPTEK) as does the HLNC-II. The deadtime coefficient $\delta$ is given by

$$\delta = (a + bT \bullet 10^{-6})\ \mu s\ ,$$

where $T$ is the measured totals rate in counts/s and $a$ and $b$ are constants given in Table III. The corrected counting rates are

**DETECTOR DEADTIME**
**(cont.)**

$$T(\text{corr.}) = T\ e^{\delta T/4}$$

and

$$R(\text{corr.}) = R\ e^{\delta T}\ .$$

It is important to use the same deadtime coefficient for both calibration and assay so that any errors in the correction will cancel to a first approximation.

At very high counting rates ($T > 1\ 000\ 000$ counts/s), a small positive bias appears in the deadtime-corrected rates as shown in Fig. 9 for PCAS-1. The bias curve was not measured for PCAS-3, but the two systems use the same predelay setting (4 μs) so we expect a similar result. A

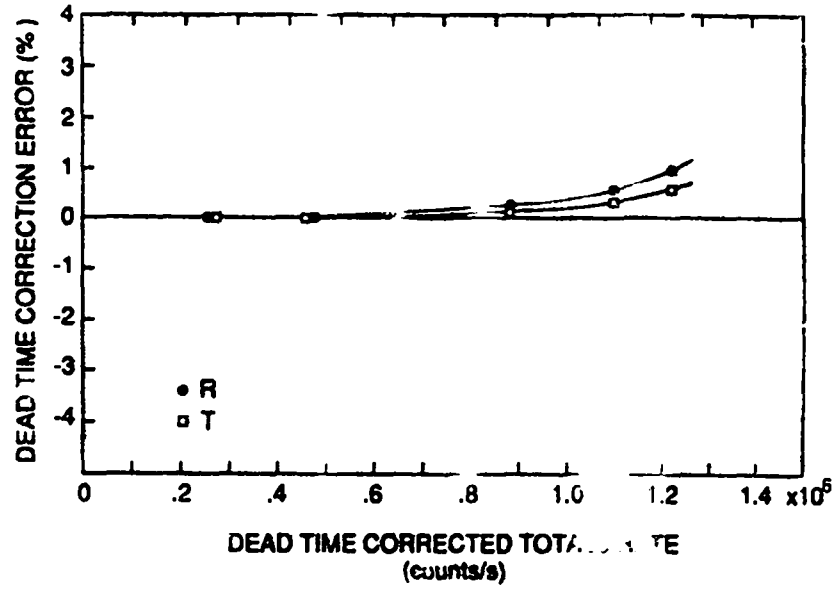


*Fig. 9. Curve showing the error in the deadtime correction for PCAS-1 at very high counting rates.*

**DETECTOR DEADTIME (cont.)**

larger predelay setting than the 4.5 μs would correct this; however, the problem is small enough to neglect.

**AXIAL RESPONSE PROFILES**

To determine sample geometry effects, a $^{252}Cf$ neutron point source was positioned at various axial locations in the sample cavity. Both totals and coincidence rates were measured at each location, and the results are shown in Fig. 10 for PCAS-3. The uniform axial-efficiency zone was obtained in the detector design by adding a polyethylene annular shim to the outside surface of the detector near the top as shown in Fig. 1. The extra polyethylene increases the neutron efficiency in the top zone. Also, cadmium absorbers were added on each tube and between the polyethylene and concrete interface in the center area to further flatten the response.

The cadmium absorbs thermal neutrons and decreases the efficiency of the $^{3}He$ tubes. Thus, the cadmium was added

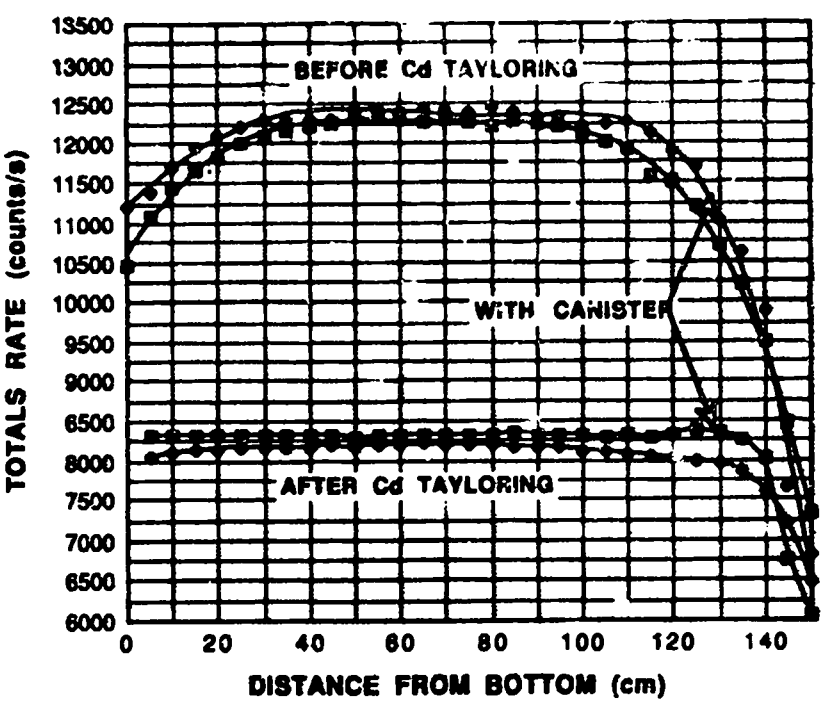


*Fig. 10. Axial efficiency profile for PCAS-3 measured with a $^{252}Cf$ source both before and after the application of the cadmium absorbers.*

**AXIAL RESPONSE PROFILES (cont.)**

to the central region to bring it into line with the two ends. Sixteen custom-designed cadmium strips were applied to the stainless steel tubes as shown in Fig. 5.

Because the canisters are filled with five or fewer separate cans, the $PuO_2$ distribution is guaranteed to be nonuniform along the axis. This makes it important to have a uniform counting efficiency. The calibration of the PCAS will be based on the multiplication-corrected reals rate $R_{mc}$ because of the heterogeneous samples and possible variable uranium content, both of which affect the multiplication. Thus, the most important response function to be uniform or flat is $R_{mc}$.

The results of the $^{252}Cf$ scan are given in Table IV, and the normalized totals profile is shown in Fig. 10. We see that the cadmium shimming reduced the central region counting efficiency by ~50% with a much smaller effect on each end. The purpose of the cadmium shimming was to extend the flat efficiency zone from about 55 cm to approximately 135 cm as shown in Fig. 10.

Figure 11 shows that the efficiency profile is flat to within ±1% over the 135-cm canister height.

The reals $R$ counting rate is shown in Fig. 12. The actual measurement will use $R_{mc}$, and the $R_{mc}$ responses are always more uniform (flat) than the reals before correction because of a built-in compensation in the multiplication correction algorithm. The magnitude of the multiplication correction decreases as the measured $R/T$ ratio decreases. Thus, near the ends of the detector where $R$ is dropping faster than $T$, the $R/T$ ratio is smaller than in the middle. This results in a smaller multiplication correction at the ends and, thus, a larger net value for $R_{mc}$ at the ends of the axial profile.

During the measurements, the canister becomes a part of the detector system, and it significantly affects the axial profile. When no canister is present, the totals rate in the

## AXIAL RESPONSE PROFILES
(cont.)

**TABLE IV.** PCAS-3 Axial Profile.

| Height (cm) | Totals ($s^{-1}$) | Reals ($s^{-1}$) |
|---|---|---|
| 5 | 8037 | 857 |
| 10 | 8102 | 883 |
| 15 | 8125 | 888 |
| 20 | 8147 | 907 |
| 25 | 8167 | 906 |
| 30 | 8170 | 889 |
| 35 | 8158 | 892 |
| 40 | 8179 | 905 |
| 45 | 8186 | 912 |
| 50 | 8177 | 891 |
| 55 | 8195 | 894 |
| 60 | 8208 | 911 |
| 65 | 8214 | 912 |
| 70 | 8206 | 885 |
| 75 | 8206 | 906 |
| 80 | 8205 | 887 |
| 85 | 8161 | 866 |
| 90 | 8168 | 901 |
| 95 | 8163 | 887 |
| 100 | 8123 | 885 |
| 105 | 8106 | 863 |
| 110 | 8081 | 882 |
| 115 | 8043 | 869 |
| 120 | 8025 | 869 |
| 125 | 7983 | 854 |
| 130 | 7962 | 850 |
| 135 | 7858 | 829 |
| 140 | 7611 | 766 |
| 145 | 7193 | 660 |
| 150 | 6479 | 520 |

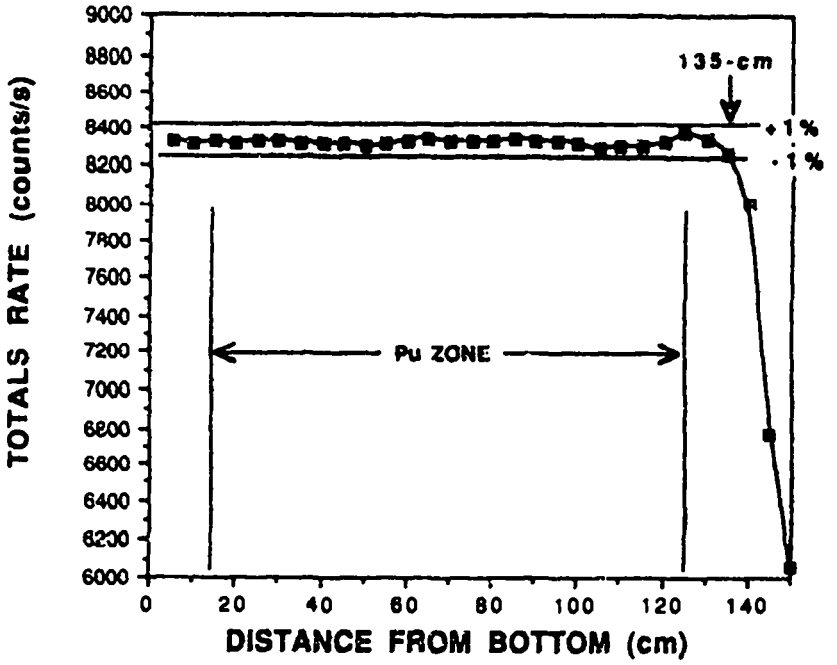


*Fig. 11. The totals rate axial profile for PCAS-3 for a $^{252}Cf$ source measured inside the dummy canister.*

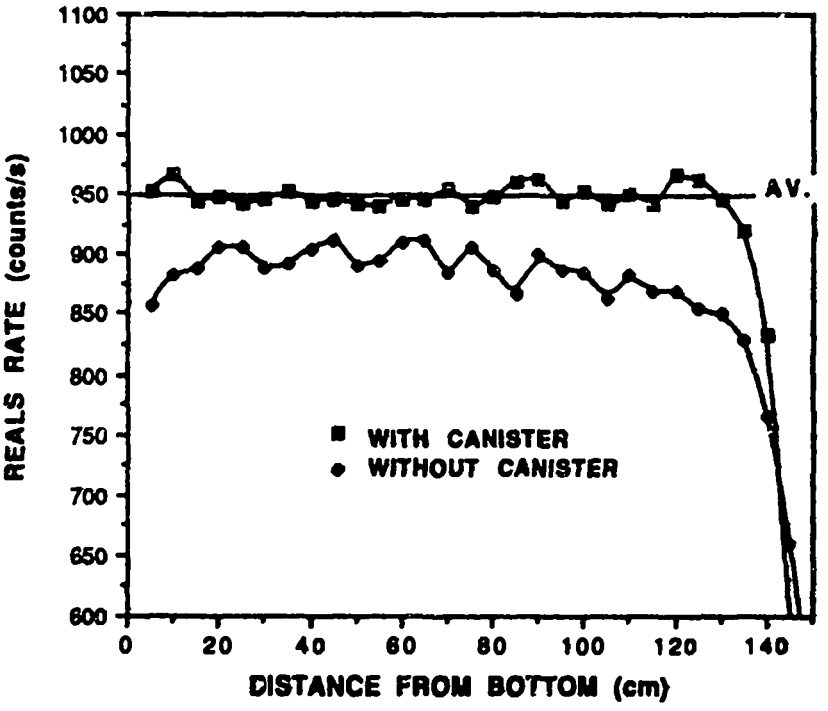


*Fig. 12. The reals counting rate as a function of height above the bottom of PCAS-3.*

**AXIAL RESPONSE PROFILES (cont.)**

bottom region decreases by ~2.5% and the rate near the top decreases by ~4% as shown in Fig. 10.

We used a dummy canister made of concentric steel pipes for the response-flattening measurements. After installation of the PCAS-3 at PFPF, we repeated the axial profile measurements using an actual double-walled canister. The measured efficiency was uniform with only a ± 0.3% standard deviation over the entire canister height.

**RADIAL RESPONSE**

To test the sensitivity of the PCAS to the radial distribution of the plutonium in the counter, we counted a $^{252}Cf$ source in the center of the detector and then recounted it at 15-mm increments to the wall. The results were uniform to better than 0.7% in the totals rate as shown in Fig. 13.

We concluded that the radial positioning of the canister and the MOX cans is not an important variable at approximately the 0.3% level.

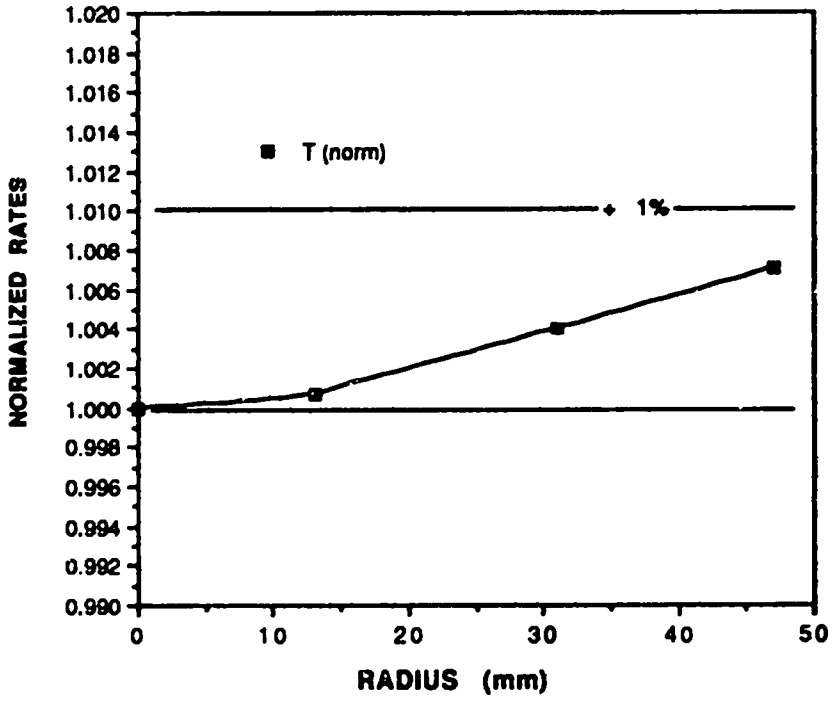


*Fig. 13. The radial efficiency profile measured with a $^{252}Cf$ source in PCAS-3.*

**SAMPLE CONTAINER**

The canister contains up to five cans of $PuO_2$ stacked on top of each other. Each can typically contains 2–2.5 kg of $PuO_2$ (~22% $^{240}Pu$).

**CAN WALL EFFECTS**

The precalibration-standard cans were of a different wall thickness and material than the PFPF cans. Measurements were performed to estimate the effect of this difference.

A $^{252}Cf$ source was placed in the center of PCAS-3 and concentric steel cans were placed around the source so we could observe the change in the counting rate. A small positive change was observed, as shown in Fig. 14. The multiplication-corrected results $R_{mc}$ are even less sensitive to the wall effects than are $R$ and $T$. Similar measurements made for PCAS-1 and the HLNC-II are shown in Fig. 14 for comparison.

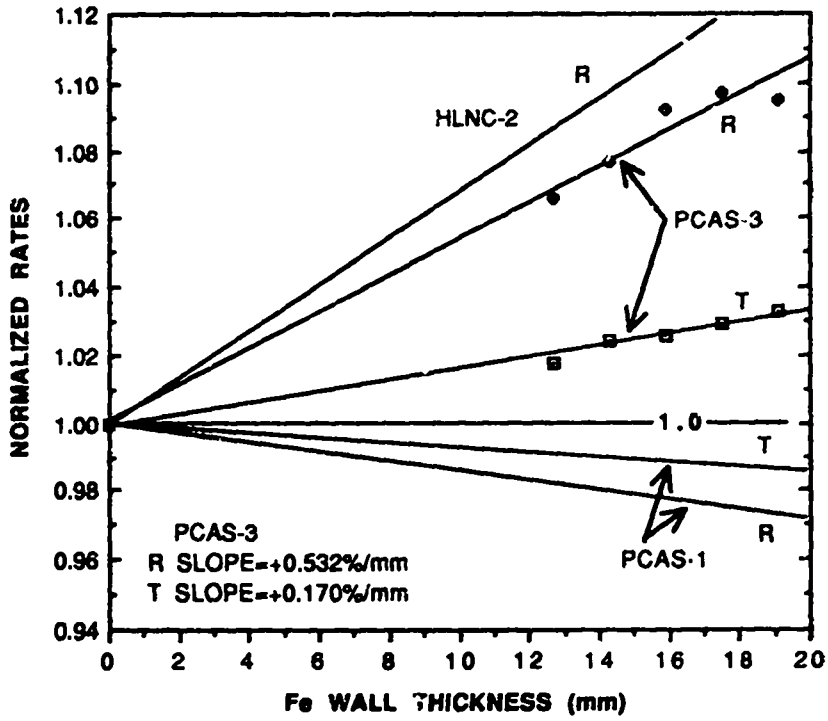


*Fig. 14. Graph showing the effect of the wall thickness of the iron container on the measured response from a $^{252}Cf$ neutron source.*

**CAN WALL EFFECTS (cont.)**

Because the final calibration is made with actual canisters and $PuO_2$ cans, no wall correction is necessary unless we compare the calibration with different types of containers.

**ROOM BACKGROUND**

The PCAS-3 operates in the continuous mode with data dumps every minute or less. The totals rate in the counter thus gives a time history of the movement of $PuO_2$ in the room or nearby areas. The PCAS-3 is unshielded, and it has an exterior surface area of about 25 000 $cm^2$, so the sensitivity is high for detecting neutron source material in the vicinity of the detector.

## GENERAL

Because PCAS-3 is operating in an unattended mode without IAEA inspectors in the facility, we designed tamper-indicating features into the nondestructive assay (NDA) system. These include the following:

- Detector head under IAEA seal,
- Unbroken cable runs between detector head and electronics cabinet,
- Sealed electronics cabinet,
- Modular electronic components that are compatible for replacement with standard IAEA equipment,
- Continuous data collection,
- Software replaceable by IAEA inspectors,
- Software diagnostics for interruption of or tampering with the signal, and
- Californium-252 check sources and normalization sources for verification of total system performance.

These measures give an in-depth redundancy in the authentication of the NDA system. Thus, the failure or removal of any particular measure does not necessarily result in the loss of overall authentication.

## SOFTWARE TESTS

The software checks the normal room-background rate and, if the level drops below a preset value, indicates the problem to the inspector.

## ACCIDENTAL TEST

The measured accidentals rates $A$ are compared at the end of every minute with the calculated accidental rates using the relationship

$$A = T^2 G \ ,$$

where $G$ is the gate length in microseconds. Any interruption or discontinuity in the signal rate will cause a failure in the comparison of the two accidental rates. This test is performed on every data point by the software, and the

| | |
|---|---|
| ACCIDENTAL TEST (cont.) | results are presented to the users (see software operations manual). |
| REALS/TOTALS TEST | Both the reals *R* and totals *T* rates are measured for all events, and the software uses the *R/T* ratio to sort out $^{252}Cf$ sources from $PuO_2$ samples. |

## PRECALIBRATION

We precalibrated the PCAS-3 at LANL before shipping the systems to Japan. Only small plutonium samples were available for the precalibration measurements. Table V lists the sample masses and coincidence rates and Fig. 15 shows the preliminary calibration. The slope of the precalibration was 8.52 counts/s • g $^{240}$Pu-eff.

**Table V.** Preliminary PCAS-3 Calibration.

| | Sample | $^{240}$Pu eff (g) | Net Total ($s^{-1}$) | Reals ($s^{-1}$) | Net Reals ($s^{-1}$) |
|---|---|---|---|---|---|
| 1 | 5 MOX pellets | 0.243 | 63.400 | 2.630 | 2.090 |
| 2 | 4 MOX pellets | 0.210 | 55.470 | 2.370 | 1.830 |
| 3 | $^{240}$Pu metal | 0.705 | 107.470 | 6.550 | 6.010 |

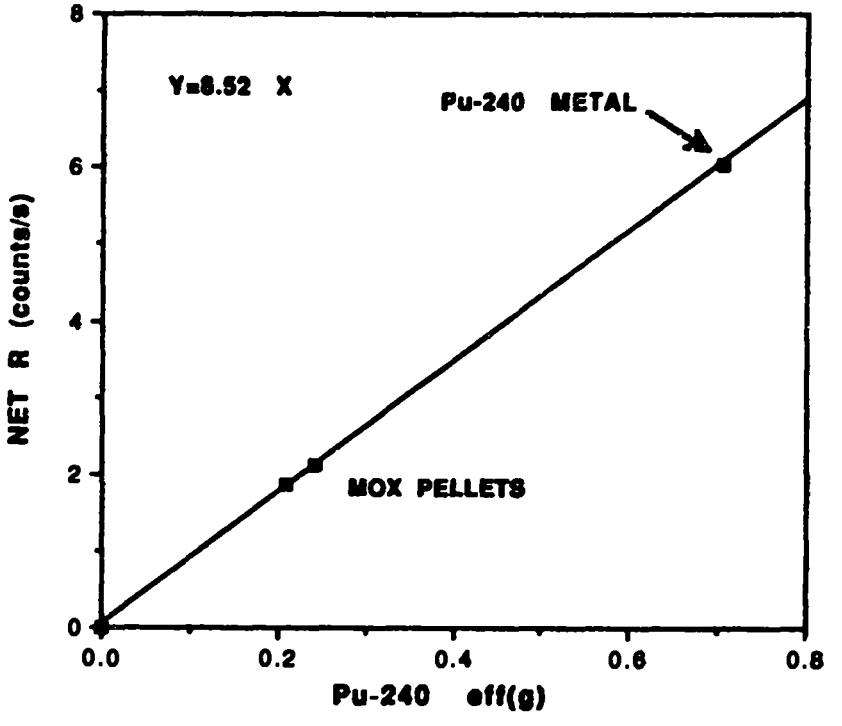


*Fig. 15. Preliminary calibration data for PCAS-3 using small non-multiplying samples of MOX and $^{240}$Pu metal.*

**PRECALIBRATION (cont.)**

The MOX pellets used in the precalibration had negligible multiplication and they were used to establish the multiplication constant $\rho_o$ as follows:

$$\rho_o = \frac{R}{T}(1+\alpha) \ ,$$

$$\rho_0 = 0.033(1+0.972) = 0.065 \ .$$

The detector PCAS-3 was physically modified between the precalibration and final calibration at the PFPF plant in that the concrete shield used at Los Alamos was not the same shield installed at PFPF.

The concrete is an integral part of the detector system (see Fig. 3), so any changes in the density can affect the detector efficiency. Measurements, using a $^{252}Cf$ normalization source at LANL and PFPF, showed that the concrete change raised the efficiency of PCAS-3 by 1.3% above the LANL precalibration value.

The change in response measured using a $^{252}Cf$ source was

$$\frac{\text{LANL shield 1}}{\text{PFPF shield 2}} = 1.013 \ \text{(Totals) and}$$

$$\frac{\text{LANL shield 1}}{\text{PFPF shield 2}} = 1.026 \ \text{(Reals)} \ .$$

The resulting change in $R_{mc}$ was 1.0%.

**PFPF CALIBRATION**

The final calibration will be performed after installation of PCAS-3 at the PFPF facility. Cans of plutonium in the canisters will be measured using PCAS-3 and subsequently sampled for destructive analysis.

**PFPF CALIBRATION (cont.)**

For future inspection purposes, the final PFPF calibration parameters will be used because the sample characteristics closely match the unknown samples. Only the multiplication-corrected results $R_{mc}$ will be used for assay because of the heterogeneous samples. The $R$ results will be collected for consistency and comparison.

## REFERENCES


1. J. E. Swansen, P. R. Collinsworth, and M. S. Krick, "Shift-Register Coincidence Electronics System for Thermal Neutron Counters," Los Alamos Scientific Laboratory report LA-8319-MS (April 1980). Also in *Nucl. Instrum. Methods* **176** (3), 555-565 (1980).

2. H. O. Menlove and J. E. Swansen, "A High-Performance Neutron Time-Correlation Counter," *Nucl. Technol.* **71**, 497-505 (November 1985).

3. H. O. Menlove, R. H. Augustson, R. Holbrooks, D. Antencio, G. Walton, S. Takahashi, T. Ohtani, M. Seya, R. Abedin-Zadeh, B. Hassan, and S. Napoli, "PFPF Canister Counter Hardware Operations and Procedures Manual," in "PFPF Canister Counter Documentation Manual" Los Alamos National Laboratory document N-1/WP-89-2 (PNC SA 0850 89-001) (1989).

4. N. Ensslin, "A Simple Self-Multiplication Correction for In-Plant Use," in *Proc. 7th ESARDA Annual Symposium on Safeguards and Nucl. Mater. Manage.* (ESARDA, Italy, 1985) **19**, pp. 233-238.


*U.S. Government Printing Office: 1993-774-036/67068